INTRODUCTION TO CURRENT AND BRIGHTNESS LIMITS

V. P. Suller
CLRC, Daresbury Laboratory, Daresbury, Warrington, Cheshire WA4 4AD, United Kingdom

1. INTRODUCTION

Current and brightness limits are potentially serious concerns for synchrotron light sources because in effect they can impose a limit on the usefulness of the source and the experimental science programmes they can cover. As will be seen, the expression for brightness contains the beam current so any limit in current automatically limits the brightness.

We will present some very simple ideas relating to beam current in electron storage rings and give an impression of the magnitudes involved by taking some examples from a range of different storage rings. Using simple expressions it will be demonstrated how the electro-magnetic fields associated with beam currents can significantly interact with the structures surrounding the beam to produce effects which can limit the current.

Then the basic equations for the brightness of synchrotron light will be stated and the factors which may limit the brightness will be explained. The brightness of two different types of source will be evaluated (for ESRF dipoles and undulators) to illustrate these factors.

2. BEAM CURRENT MEASUREMENT AND TYPICAL VALUES

The beam current in an accelerator is defined in the same way as a normal electric current, that is, the rate at which charge passes a fixed point. It can be measured by two different techniques, as shown in fig 1:-

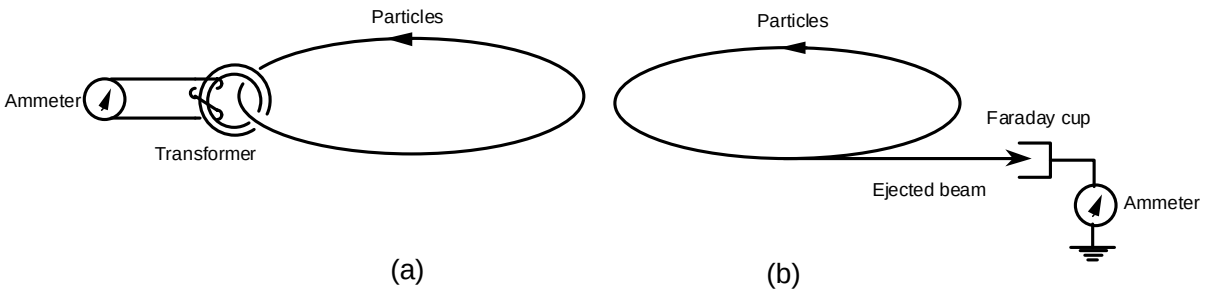

Fig 1
(a) DC current transformer (this measures the magnetic field produced by the current)[1]
(b) Faraday cup (this measures the total beam charge and needs the beam to be ejected)[2]

Notice that the two methods will give greatly differing results for the same number of particles (see below).

If there are N particles of charge q moving with velocity v in a circular accelerator of circumference $2\pi R$, the current transformer will indicate a circulating beam current I_0

$$I_0 = \frac{Nqv}{2\pi R}$$

If we restrict our view to synchrotron radiation sources with electrons at relativistic (v = c) velocity this expression becomes

$$I_0 = \frac{Nec}{2\pi R} \text{ or } = Nef_0$$

where e is the electronic charge and f_0 is the orbit frequency.

Note that if the same beam were ejected into a Faraday Cup it would indicate

$$I_{fc} = Nef_{rep}$$

where f_{rep} is the repetition rate of the accelerator.

$$\frac{I_0}{I_{fc}} = \frac{f_0}{f_{rep}}$$

This ratio is typically a very large number since f_0 is usually MHz and f_{rep} is Hz, so that in the example of the ISIS[3] spallation source accelerator where a high current of 800 MeV protons is ejected at 50 Hz, the faraday cup indicates an average current of 200 μA whereas a current transformer would show 6 Amperes for the circulating beam current.

The circulating beam current is determined both by the number of electrons and by the circumference, as is seen in these examples:-

	$2\pi R$(m)	I_0 mA	N
HELIOS[4]	9.6	300	$6.0\ 10^{10}$
ESRF[5]	844	200	$3.5\ 10^{12}$
LEP[6]	$26.7\ 10^3$	6 (8x $^3/_4$ mA)	$3.3\ 10^{12}$

The small circumference of HELIOS produces a relatively high current with few electrons, whilst even the large number of electrons in the large circumference of LEP does not produce a big current.

The beam current transformer measures the average current as if the electrons were uniformly spread around the circumference. In reality they are in a bunch train imposed by the Radio Frequency accelerating system. The harmonic number h is the maximum number of bunches around the circumference.

$$h = \frac{2\pi R}{\lambda_{rf}} = \frac{f_{rf}}{f_0}$$

The bunches typically have a gaussian structure in time, as shown in fig 2, where the length of the bunches is often described by the full width at half maximum (fwhm) of the peak. This may be conveniently expressed in terms of a fraction k of the period of the RF [7]

$$\text{fwhm} = 2.36\sigma_t = k\frac{1}{f_{rf}}$$

Normally k will have a value between 0.01 and 0.1, depending on the storage ring design. From the well known properties of gaussians we can relate the peak current I_{pk} to the average I_0

$$\sqrt{2\pi}\sigma_t I_{pk} = \frac{I_0}{f_{rf}} \quad I_{pk} = 0.94\frac{I_0}{k}$$

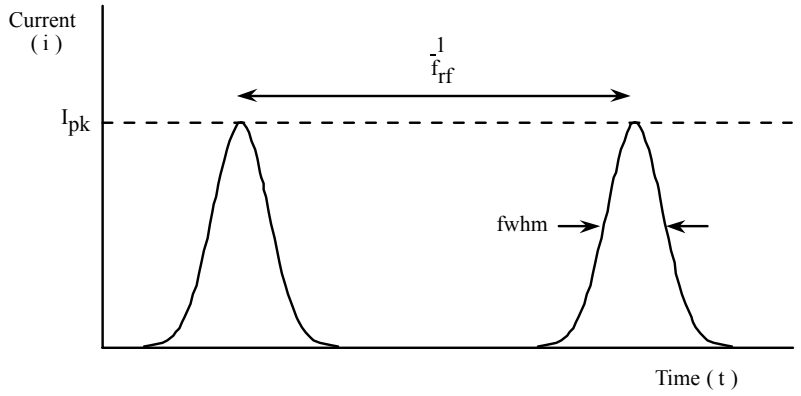

Fig 2 Time structure of the bunches

With the value for k in storage rings typically being between 0.1 and 0.01 it can be easily seen that the peak current can be 10 to 100 times higher than the average current. Even higher peak currents are produced when electron storage rings operate, as is often the case, with the beam current concentrated in a single (or few) bunches. The current transformer will still register a reading $I_{0(sb)}$ as though the electrons are spread around the circumference, but the peak current is increased by a factor of the harmonic number h because now:-

$$\sqrt{2\pi}\sigma_t I_{pk} = \frac{I_{0(sb)}}{f_0}$$

$$I_{pk} = 0.94h\frac{I_{0(sb)}}{k}$$

Consider these examples of peak currents in storage rings operated in single or few bunch mode, from which it can be seen that peak currents can easily reach values of hundreds of amperes.

	$I_{0(sb)}$(mA)	k	f_o	h	N	I_{pk} Amps
SRS[8]	100	0.11	$3.1\ 10^6$	160	$2.0\ 10^{11}$	136
ESRF[9]	10	0.03	$3.5\ 10^5$	992	$1.8\ 10^{11}$	310
LEP[10]	$^3/_4$	0.025	$1.1\ 10^4$	31360	$4.3\ 10^{11}$	885

It is not surprising that the electro-magnetic fields associated with these very high peak currents can produce effects which destabilise the electron bunches and produce current limitations.

3. FOURIER COMPONENTS OF THE BEAM CURRENT

Consider the time structure of the beam current in more detail. The train of bunches in the beam current, as shown in fig 2, can be expressed as a Fourier series:-

$$i(t) = \frac{a_0}{2} + \sum_{n=1}^{\infty} a_n \cos n\omega t + \sum_{n=1}^{\infty} b_n \sin n\omega t$$

To allow the coefficients of this series to be estimated by inspection, a simplifying assumption can be made that the bunches are rectangular in time with length k/f_{rf} and height I_{pk} and by setting the origin of the time axis at the centre of a bunch, all the coefficients b_n are zero. The interval between bunches $1/f$ is (yet) an unspecified number of rf periods.

The coefficients of the series are evaluated

$$a_n = \frac{1}{\pi} \int_o^{2\pi} i(t) \cos n\omega t . d(\omega t)$$

and describe the amplitudes of the different frequencies present in the beam current. We evaluate a_0 with n = 0 thus

$$\begin{aligned} a_0 &\approx \frac{1}{\pi} I_{pk}\, 2\pi f \frac{k}{f_{rf}} \\ &\approx 2 I_{pk} k \frac{f}{f_{rf}} \\ &\approx 2 I_0 \end{aligned}$$

and $a_0/2$ gives the expected amplitude for the steady component of the beam current.

The question "Which value of n gives a zero for the coefficient a_n ?" can be answered approximately by inspecting the product of the beam current function and the cosine term in the integral. It will give an indication of the highest frequency component present. The coefficient will be zero when

$$n\omega \frac{k}{2f_{rf}} = \pi$$

$$n = \frac{1}{k}\frac{f_{rf}}{f}$$

The value of f is determined by the interbunch spacing and we can consider two limiting situations.

In multibunch	$f = f_{rf}$
In singlebunch	$f = f_0$

But in both these cases the actual frequency nf at which the coefficient goes to zero is the same, namely

$$= \frac{f_{rf}}{k}$$

The beam current spectrum is therefore a series extending to at least 10 to 100 times the radio frequency. In multibunch the series ($n = 1/k$) is at intervals of f_{rf} but in singlebunch there are many more harmonics ($n = h/k$), at intervals of the orbit frequency f_0.

Some limitations of beam current and brightness arise from the interaction between the components of this spectrum and the accelerator environment in which the beam current circulates.

4. FIELDS OF RELATIVISTIC ELECTRONS

Consider the fields surrounding an electron. If the electron is stationary there is only a uniformly symmetric electric field shown in fig 3. At a radius r the magnitude of the electric field can quickly be calculated using Gauss' Law

$$\oint E.ds = \frac{e}{\varepsilon_0} \qquad \varepsilon_0 \text{ is the permittivity of free space}$$

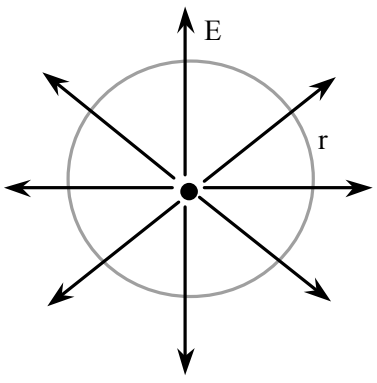

Fig 3 Electric field surrounding a stationary electron

The integral is made over the surface of a sphere at radius r, thus

$$E.4\pi r^2 = \frac{e}{\varepsilon_0}$$

$$E = \frac{1}{4\pi\varepsilon_0}\frac{e}{r^2}$$

If the electron is moving relativistically with respect to an observer the electric field suffers a relativistic contraction along the line of motion. For an electron moving with velocity βc with $\gamma = \sqrt{1-\beta^2}^{-1}$ the electric field seen by the observer at rest is as shown in fig 4.

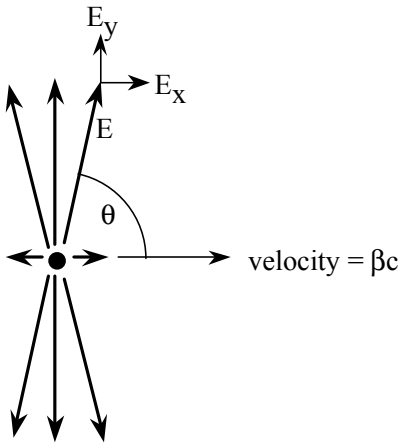

Fig 4 Electric field of a relativistic electron

The x direction is along the axis of the electron's motion, while the y direction is perpendicular to it. The general expressions for the electric field components are [11]

$$E_x = \frac{\gamma\cos\theta}{(1+(\gamma^2-1)\cos^2\theta)^{3/2}}\cdot\frac{e}{4\pi\varepsilon_0 r^2}$$

$$E_y = \frac{\gamma\sin\theta}{(1+(\gamma^2-1)\cos^2\theta)^{3/2}}\cdot\frac{e}{4\pi\varepsilon_0 r^2}$$

If these expressions are examined for two extreme values of θ
Along the axis of motion at $\theta = 0$

$$E_y = 0, \qquad E_x = \frac{1}{\gamma^2}\frac{e}{4\pi\varepsilon_0 r^2}$$

Within a small angle to the normal to the axis of motion at $\theta = \frac{\pi}{2} - \frac{1}{\gamma}$

$$E_y = \frac{\gamma}{2^{3/2}}\cdot\frac{e}{4\pi\varepsilon_0 r^2} \qquad E_x = \frac{1}{2^{3/2}}\cdot\frac{e}{4\pi\varepsilon_0 r^2}$$

Because γ has a large value for relativistic electrons, it can be seen that the only significant field component is within $\pm\frac{1}{\gamma}$ of the normal to the electron motion. Thus the electric field is concentrated into a disc of angular thickness $\pm\frac{1}{\gamma}$ at right angles to the electron's motion as shown in fig 5

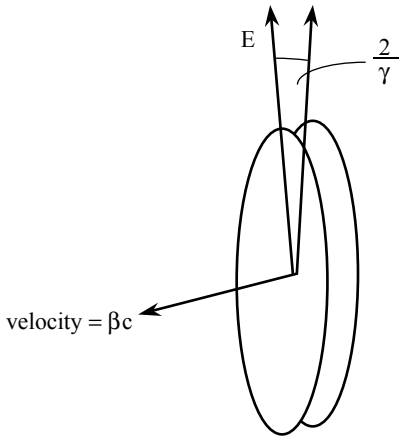

Fig 5 The electric field of a relativistic electron is concentrated into a disc at right angles to the velocity.

Using this concept of the field concentrated into a disc we can quickly confirm (approximately) the result above by using Gauss' Law over the edge of the disc

$$\oint E ds \approx E_y 2\pi r.\frac{2r}{\gamma} = \frac{e}{\varepsilon_0}$$

$$E_y = \gamma\frac{e}{4\pi\varepsilon_0 r^2}$$ (compare to the exact treatment above)

The moving charge also appears as a current i to the stationary observer. If we consider this current to be the passage of charge e in the time $\frac{2r}{\gamma c}$ which the disc edge takes to pass the observer, then

$$i = \frac{e\gamma c}{2r}$$

Using Ampere's law for the magnetic field surrounding a current

$$\oint B dl = \mu_0 i \qquad \mu_0 \text{ is the permeability of free space}$$

$$B2\pi r = \mu_0\frac{e\gamma c}{2r}$$

$$B = \frac{\gamma \mu_0}{4\pi r^2} ec$$

Since $\varepsilon_0 \mu_0 = \frac{1}{c^2}$, we have the expected relation between the magnetic and electric fields;

$$B = E/c$$

5. EFFECTS DUE TO THE VACUUM CHAMBER WALLS

It has been shown that a relativistic electron has its electric field concentrated into a disc. When the electron is moving within the conducting vacuum chamber of an accelerator the disc must terminate at the chamber wall on an opposite sign image charge moving along with the electron.

If the walls are not perfectly conducting the image charge will dissipate energy in the walls; this is a resistive wall effect. However, the energy dissipation is usually negligible. For example, a 1000 m circumference accelerator with a vacuum chamber made of stainless steel would have a resistance of about 1 Ω. Applying Ohm's Law to a 300 mA image current flowing in this resistance gives a dissipation of only 0.1 W. The high frequency components of the beam current see a higher resistance due to the skin effect but again the dissipation is usually not important.

The resistive loss in the chamber walls can be pictured as a longitudinal drag force on an electron bunch and as such does not cause any stability problems for the bunch. If the bunch is not aligned transversely with the axis of the vacuum chamber the transverse asymmetry of the electric field disc can be expected to produce a transverse force component and this can lead to an instability. This is called the transverse resistive wall instability [12].

In addition to resistance the vacuum chamber walls can show other [13] electrical impedance properties, that is, capacitance or inductance. These arise from changes in the geometrical shape of the vacuum chamber, as seen by the fields surrounding the beam. As the beam moves at relativistic velocity from a region with one shape of the chamber to another, both the fields and the image currents become distorted and can even be left in these shape changes 'ringing' behind the beam. These residual fields can then interact with the tail of the bunch, or with beam bunches which pass later (even with the same bunch on a later orbit), and are the principal reason for the existence of beam current and brightness limitations.

Even though the capacitances and inductances resulting from shape changes in the vacuum chamber are quite small (a 10 mm step in a 100 mm diameter pipe contributes an inductance of order 0.01 μHenries [14]) it must be remembered that the peak current in the bunch may exceed hundreds of amperes. In the chamber impedance such a bunch can produce fields equivalent to hundreds of volts and this is sufficient to affect the stability of the bunches.

When the field from the head of a bunch affects the tail of the same bunch this is called a single bunch effect. [15]

When the field of a bunch affects later bunches this is called a multi bunch effect. [15]

The observable effects may be:

1. Bunch position oscillations (transverse or longitudinal)
2. Bunch shape oscillations (" ")
3. Bunch size changes (" ")

All these effects, which originate in the electromagnetic fields generated by the beam in the vacuum chamber, may be described by a general impedance function. [13] This is usually expressed as an impedance containing two different contributions:

I. A broadband impedance (hence low Q-factor) representing the total effect of the wall resistance (including skin effects) together with capacitive and inductive terms arising from all the geometrical effects of dimension changes, branches, tees, slots, etc.

II. Several (perhaps many) narrow band (hence high Q-factor) impedances due to resonant structures in the chamber such as RF cavities.

The broadband resonator impedance is a shunt arrangement shown in fig 6 representing the longitudinal chamber impedance Z_{II}.

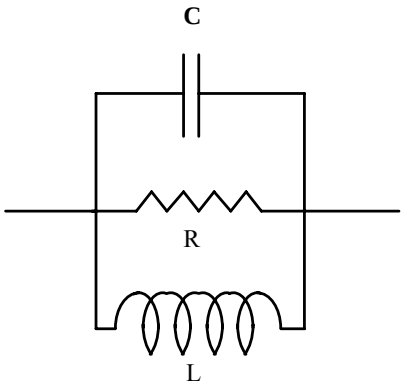

Fig 6 Components of the broadband longitudinal chamber impedance Z_{II}.

The most useful formula used is:

$$Z_{II} = \frac{R}{1 + jQ\left(\frac{\omega_{res}}{\omega} - \frac{\omega}{\omega_{res}}\right)}$$

$$\omega_{res} = \frac{1}{\sqrt{LC}}, \qquad Q = R\sqrt{\frac{C}{L}}$$

Remembering that the beam spectrum extends up to many times the RF, and that at a frequency of several Ghz most vacuum chambers start to propagate like a waveguide, it is to be expected that ω_{res} will be in the Ghz region.

To obtain a suitably broadband response over this range Q must be of the order ~1.

For Q=1, Z_{II} has the following Real and Imaginary parts, as shown in fig 7.

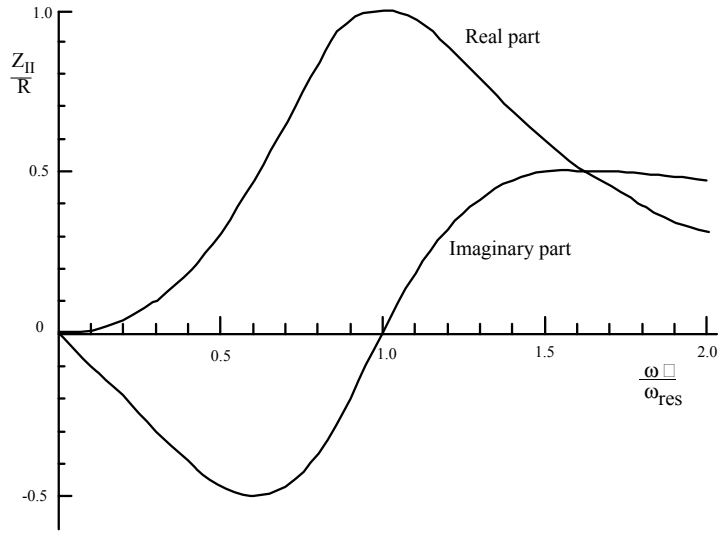

Fig 7 Real and Imaginary components of the broadband impedance.

The important Impedance parameter in single bunch instabilities is

$$\frac{Z_{II}}{n}, \qquad \text{where } n = \frac{\omega}{\omega_o}$$

This effectively normalises between accelerators of different circumference. For modern light source accelerators which need to operate with good beam quality at several hundred mA it is generally accepted that the magnitude [16]

$$\frac{Z_{II}}{n} \leq 1 \ \Omega$$

Examples of measured $\frac{Z_{II}}{n}$ in light sources:

SRS 1.8 ± 0.6 Ω	[8]
ALS 0.2 Ω	[17]
LEP 0.25-0.5 Ω	[18]

It is intuitively apparent that a beam moving off centre down the vacuum chamber will generate different fields than a beam which is centred. This must imply that there is a transverse component $Z_\perp$ to the chamber impedance, although it is closely related to the longitudinal impedance Z_{II}.

The generally used approximate relationship between them is [19]:

$$Z_{\perp} = \frac{Z_{II}}{n}\frac{2R}{b^2}$$

where R is the accelerator average radius and b is the radius of the vacuum chamber aperture. Note that the dimensions of $Z_{\perp}$ are Ω/m.

The mathematical treatment of instabilities is well beyond the scope of this paper. The concepts which have already been introduced, however, can be appreciated for the role that they play in the behaviour of instabilities.

An expression for the growth rate of some coordinate of a theoretical test particle within the beam can be derived [19], which is related to the beam current and the chamber impedance. An instability will not necessarily develop on all occasions because there are often damping mechanisms (by synchrotron radiation emission [20] or by Landau damping [21], for example) which stifle the instability because the damping rate exceeds the growth rate. But since the growth rate is related to the beam current, above some threshold current the instability will grow. Even then the growth may stabilise at a new equilibrium because of frequency shifts with amplitude and Landau damping.

Thus below the instability threshold current the beam will exhibit its theoretical dimensions, whereas above the threshold the beam may grow to an increased size, or oscillate, or suffer an intensity reduction until it restabilises below the threshold. All these behaviours are obviously important to users of synchrotron radiation facilities.

6. BRIGHTNESS OF A SYNCHROTRON RADIATION SOURCE

The usefulness of a synchrotron radiation source may be judged by an experimenter primarily in terms of how many photons per second can be directed onto the sample. The relevant factors which influence this are the emission properties of the source and the acceptance parameters of the beamline, the optics, the detectors and the sample itself. Ideally there should be a good match between the emission and the acceptance.

The long established radiometric parameter which describes this emission property of a source of radiation is called the Brightness, although the term Radiance or Illuminance may sometimes be used.[22] Spectral Brightness is defined at a particular photon wavelength as the radiated flux per unit area of the source and per unit solid angle of emission.

$$\text{Spectral Brightness} = \frac{d^4F}{dx\,dz\,d\theta\,d\varphi} \quad \text{photons/sec/mm}^2\text{/mr}^2\text{/0.1\%bandwidth}$$

where dF is the radiated photon flux in a narrow 0.1% bandwidth, over which it can be assumed that the flux does not vary. The coordinates are as defined in fig 8.

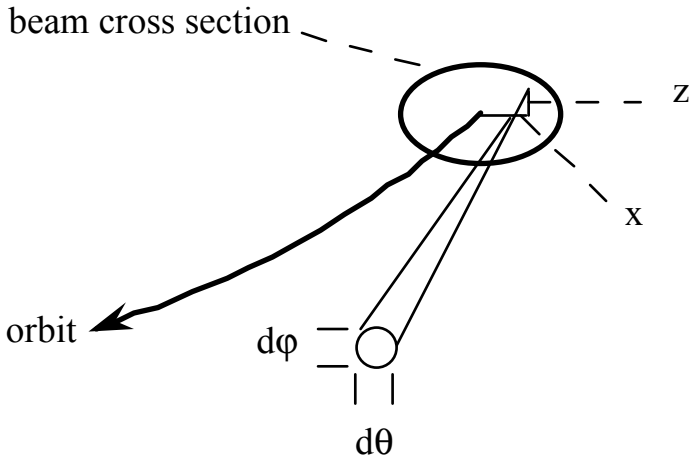

Fig 8 Coordinates used in defining source properties.

Notice that Brightness, as defined above, in Europe is sometimes referred to as Brilliance [23], with an accompanying incorrect use of the term brightness for the Spectral Flux Intensity. The author prefers to avoid confusion by using the established radiometric definitions as given above, which is also the practice in the USA.

If dF is integrated over all wavelengths a simple expression gives the total power in the synchrotron radiation spectrum:-

$$\text{Power(kW)} = \frac{88.5\,\text{E}^4\text{(GeV)}\text{I}_0\text{(A)}}{\text{R(m)}}$$

where E is electron energy, I_o is beam current (average) and R is bending radius

Examples:

	E(GeV)	I_0(A)	R(m)	Power(kW)
HELIOS[24]	0.7	0.3	0.52	12.3
SRS[25]	2.0	0.3	5.55	76.5
ESRF[26]	6.0	0.2	23.3	985
LEP[10]	50.0	0.006	3096	1072

The synchrotron radiation spectrum is described with reference to a characteristic (often called 'critical') wavelength λ_c, or photon energy ε_c

$$\lambda_c(\text{Å}) = \frac{5.59\text{R(m)}}{\text{E}^3\text{(GeV)}} = \frac{18.6}{\text{B(Tesla)E}^2\text{(GeV)}}$$

$$\varepsilon_c(\text{keV}) = \frac{12.39}{\lambda_c(\text{Å})}$$

where B is the bending magnetic field.

Examples:

	E(GeV)	R(m)	B(T)	λ_c(Å)	ε_c(keV)
BESSY-I[27]	0.8	1.78	1.5	19.4	0.64
HELIOS[28]	0.7	0.52	4.5	8.5	1.5
SRS[25]	2.0	5.55	1.2	3.9	3.2
ESRF[29]	6.0	23.3	0.86	0.60	20.7
LEP[30]	50.0	3096	0.054	0.14	88.5

When the radiation at a given wavelength is integrated over all angles of vertical emission the resultant Spectral Flux Density is given by

$$\frac{dF}{d\theta} = 2.46\,10^{13}\, I_0(A)E(GeV)\left(\frac{\lambda}{\lambda_c}\right)^2 G\left(\frac{\lambda}{\lambda_c}\right) \quad \text{photons/sec/mr/0.1\% bandwidth}$$

where $G\left(\frac{\lambda}{\lambda_c}\right)$ [31] is a numerical factor which essentially governs the shape of the spectrum.

Note that source Brightness as defined above is a function whose value depends on the source density distribution and on the observation angle. It is often more convenient to use, as a figure of merit, an average brightness which for dipole sources is defined [32]:

$$\text{Average Spectral Brightness} = \frac{\frac{dF}{d\theta}}{2.36\sigma_x 2.36\sigma_z 2.36\sigma'_\gamma}$$

where $\frac{dF}{d\theta}$ is the vertically integrated flux, $2.36\sigma_x$ is the fwhm of the horizontal electron beam size, $2.36\sigma_z$ is the fwhm of the vertical electron beam size, and $2.36\sigma'_\gamma$ is the fwhm of the photon emission angle in the vertical plane. The latter is a combination of the electron beam vertical divergence and the photon emission angle thus

$$\sigma'_\gamma = \sqrt{\sigma'^2_z + 0.41\left(\frac{\lambda}{\lambda_c}\right)\frac{1}{\gamma^2}}$$

As an example let us calculate the Average Brightness of a dipole magnet in the ESRF [23]

General data	Source point data	Electron beam data	At $\lambda = \lambda_c$
E = 6 GeV			
I_0= 200 mA	β_x = 1.0 m	σ_x = 0.07 mm	λ_c = 0.6 Å
ε_x= 4 10^{-9} m.rads	β_z = 25.0 m	σ_z = 0.032 mm	σ_γ' = 0.055 mr
ε_z= 4 10^{-11} m.rads	η = 0.03 m	σ_z' = 0.0013 mr	
σ_E = 10^{-3}			

$$\frac{dF}{d\theta} = 2.46\ 10^{13}\ 0.2\ 6\ 0.65 \quad \text{at } \lambda = \lambda_c$$

$$= 1.9\ 10^{13} \text{ photons/sec/mr/0.1\% band}$$

$$\text{Dipole Average Spectral Brightness} = \frac{1.9\,10^{13}}{2.36^3\ 0.07\ 0.032\ 0.055}$$

$$= 1.2\ 10^{16} \text{ photons/sec/mm}^2\text{/mr}^2\text{/0.1\% band}$$

The brightness performance of an undulator is calculated slightly differently. The flux in the central cone of an undulator F_n at a specified wavelength is averaged over the emission angle of that cone to give the Average On-axis Brightness. Because of the usually very small source size and divergence in an undulator diffraction effects must be taken into account. [33]

$$\text{Average On-axis Brightness} = \frac{F_n}{2.36^4 \sigma_{\gamma x} \sigma'_{\gamma x} \sigma_{\gamma z} \sigma'_{\gamma z}} \quad \text{photons/sec/mm}^2\text{/mr}^2\text{/0.1\% band}$$

where $\sigma_{\gamma z}$, $\sigma_{\gamma z}$ are the photon source sizes in both planes and $\sigma_{\gamma z}'$, $\sigma_{\gamma z}'$ are the photon source divergence in both planes, taking into account diffraction effects.

$$\sigma_{\gamma x,z} = \sqrt{\sigma_{x,z}^2 + \sigma_\gamma^2} \qquad \sigma_\gamma = \frac{1}{4\pi}\sqrt{\lambda_n L}$$

$$\sigma'_{\gamma x,z} = \sqrt{\sigma'^2_{x,z} + \sigma'^2_\gamma} \qquad \sigma'_\gamma = \sqrt{\frac{\lambda_n}{L}}$$

where L = undulator length, λ_u = undulator period

The standard expression for the radiation produced in the n^{th} harmonic in an undulator is

$$\lambda_n = \frac{\lambda_u}{n2\gamma^2}\left(1+\frac{k^2}{2}\right)$$

where the deflection parameter $k = 93.4\ \lambda_u(m)B_o(Tesla)$

and the flux in the central cone is [34] $F_n=1.43\ 10^{14}\ \frac{L}{\lambda_u}\ I_0\ Q_n(k)$ photons/sec/0.1% bandwidth

where

$$Q_n(k) = \left(1+\frac{k^2}{2}\right)\frac{f_n}{n}$$

and f_n is a numerical factor, related to k. [35]

As an example let us calculate the On-axis Brightness of an ESRF undulator [36]

General data	Source point data	Electron beam data	Photon data
$\lambda_u = 46$ mm N = 36 L = 1.66 m $\gamma = 1.17\ 10^4$	$\beta_x = 0.5$ m $\beta_z = 4.0$ m $\eta = 0.04$m	$\sigma_x = 0.06$ mm $\sigma_x' = 0.12$ mr $\sigma_z = 0.013$ mm $\sigma_z' = 0.003$ mr	$\sigma_\gamma = 0.0016$ mm $\sigma_\gamma' = 0.012$ mr $\sigma_{\gamma x} = 0.06$ mm $\sigma_{\gamma x}' = 0.12$ mr $\sigma_{\gamma z} = 0.013$ mm $\sigma_{\gamma z}' = 0.012$ mr

Consider k = 1, then the wavelength of the fundamental is

$$\lambda = \frac{46\ 10^{-3}}{2\left(1.17\,10^4\right)^2}\left(1+\frac{1}{2}\right) = 2.5\ 10^{-10}\ \text{m}$$

$$F_n = 1.43\,10^{14}\ 36\ 0.2\ \frac{3}{2}\ 0.37$$
$$= 5.7\,10^{14}\ \text{photons / sec/ 0.1\% band}$$

$$\text{On-axis Brightness} = \frac{5.7\,10^{14}}{2.36^4\ 0.06\,0.013\,0.12\,0.012}$$

$$= 1.6\ 10^{19}\ \text{photons/sec/mm}^2\text{/mr}^2\text{/0.1\% band}$$

7. BRIGHTNESS LIMITATIONS

It has been shown that the brightness of a synchrotron radiation source depends on the beam current and the cross sectional dimensions of the beam itself. Both these quantities may be degraded by effects arising from the impedance behaviour of the beam vacuum chamber; the beam may be limited to a threshold current; or above it the beam dimensions may increase. The end result is to limit the brightness properties of the source.

These are what might be called technological limitations, which may be overcome by appropriate designs to ensure a suitably low impedance. Alternatively, feedback systems may be employed to counteract specific instabilities.

But as the technological design of synchrotron sources moves steadily towards the achievement of yet smaller beam dimensions, the ultimate limit will then be reached when, no matter how small the beam is, diffraction effects predominate. Until that happy day for experimentalists is reached, there remains much to be done by accelerator theorists, scientists and technicians.

REFERENCES

[1] K Unser; IEEE Trans Nuc Sci, NS-16,p934, (1969)

[2] KL Brown and GW Tautfest; Rev Sci Instr, 27, p696, (1956)

[3] ISK Gardner; Proc 1st European Part Accel Conf, Rome 1988, p65

[4] VC Kempson et al; Proc 4th European Part Accel Conf, London 1994, p594

[5] JM Filhol; Proc 4th European Part Accel Conf, London 1994, p8

[6] E Keil; Proc 3rd European Part Accel Conf, Berlin 1992, p22

[7] RP Walker; Proc CERN Accel School, Juvaskula 1992, CERN 94-01, p485

[8] JA Clarke; Proc USA Part Accel Conf, Dallas 1995, p3128

[9] JL Revol and E Plouviez; Proc 4th European Part Accel Conf, London 1994, p1506

[10] B Zotter; Proc 3rd European Part Accel Conf, Berlin 1992, p273

[11] Richtmeyer, Kennard and Lauritsen; Introduction to Modern Physics, 5th edition, p73, McGraw-Hill 1955

[12] LJ Laslett et al; Rev Sci Instr, 36, p436, (1965)

[13] M Furman et al; Chapter 12 in Synchrotron Radiation Sources, a Primer; H Winick(ed), World Scientific 1994

[14] SA Heifets and SA Kheifets; Revs Mod Phys, 63, p631, (1991)

[15] A Hofmann; Proc 11th Int Conf High Energy Accel, p540, Geneva 1980

[16] M Cornacchia; Proc CERN Accel School, Chester 1989, CERN 90-03, p68

[17] JM Byrd and JN Corlett; Proc 4th European Part Accel Conf, London 1994, p1069

[18] D Brandt et al; Proc 2nd European Part Accel Conf, Nice 1990, p240

[19] JL Laclare; Proc 11th Int Conf High Energy Accel, p526, Geneva 1980

[20] RP Walker; Proc CERN Accel School, Juvaskula 1992, CERN 94-01, p461

[21] HG Hereward; Proc CERN Accel School, Oxford 1985, CERN 87-03, p255

[22] Jenkins and White; Fundamentals of Optics, 3rd edition, p108, McGraw-Hill 1957

[23] JM Lefebvre; Proc 5th European Part Accel Conf, Sitges 1996, p67

[24] RJ Anderson et al; Proc 3rd European Part Accel Conf, Berlin 1992, p187

[25] VP Suller et al; Proc 1st European Part Accel Conf, Rome 1988, p418

[26] A Ropert; Proc 3rd European Part Accel Conf, Berlin 1992, p35

[27] D Einfeld and G Muelhaupt; Nuc Instr Meth , 172, p55, (1980)

[28] MN Wilson; Proc 2nd European Part Accel Conf, Nice 1990, p295

[29] M Lieuvin et al; Proc 3rd European Part Accel Conf, Berlin 1992, p1347

[30] K Huebner; Proc CERN Accel School, Chester 1989, CERN 90-03, p32

[31] GK Green; Brookhaven National Laboratory Report, BNL 50522, 1976

[32] KJ Kim; Nuc Instr Meth Phys Res,A246, p71, (1986)

[33] S Krinsky; IEEE Trans Nuc Sci, NS-30, p3078, (1983)

[34] KJ Kim; Section 4 in X-Ray Data Booklet, Lawrence Berkeley Laboratory report, PUB-490, 1985

[35] European Science Foundation report 'European Synchrotron Radiation Facility; supplement II, The Machine', p56, (1979)

[36] L Farvacque et al; Proc 5th European Part Accel Conf, Sitges 1996, p632